On the Gunn Effect in GaAs HBTs

M. Rudolph, R. Doerner, and P. Heymann
Ferdinand-Braun-Institut für Höchstfrequenztechnik,
Albert-Einstein-Str. 11, D-12489 Berlin, Germany

Abstract— **A negative RF-resistance effect in GaAs HBTs is described. It results from the non-linear velocity – field characteristic in GaAs, takes place in the bulk collector, and leads to $|S_{22}|$ exceeding unity. Dependence on bias point and collector doping, and consequences for modeling are discussed.**

I. Introduction

The electron-velocity – field characteristic in bulk GaAs is nonlinear, with a negative slope at high fields. This leads to negative differential resistances and finally to the formation of Gunn domains, which is used in transferred electron devices (TEDs) to generate oscillations. In order to make the Gunn effect possible, length L and electron density n of bulk GaAs must satisfy the following condition [1]:

$$L \times n > 1 \cdot 10^{12}\text{cm}^{-2} \quad (1)$$

The second requirement is an electric field large enough to transfer electrons to satellite valleys. In GaAs, $E > 3.2$ kV/cm is required. In resistive bulk material, this condition can be expressed in terms of the current density J_G and doping N_c [2]:

$$J_G = qv_sN_c \quad (2)$$

with electron charge q and the electron saturation-velocity v_s.

These conditions can be satisfied not only in TEDs, but also in GaAs-based transistors. In GaAs MESFETs, for example, it has been found that a negative resistance observed in the drain-source channel can lead to $|S_{22}| > 1$, and even Gunn oscillations have been reported [2], [3].

Regarding GaAs HBTs, such effects can occur in the collector region. Under low-injection, however, Gunn effect is not observed, since the carrier concentration n is too low in the space-charge region, and thus eq. (1) is not satisfied. In the non-depleted (ohmic) collector region, on the other hand, the electric field is caused by the collector current J_c that is lower than J_G given by (2). Even under high-injection conditions, as is pointed out in a theoretical study [4], formation of Gunn domains is unlikely to happen in usual HBT structures with uniformly doped collector, since the base push-out (Kirk) effect will set in approximately at the current density J_G [5]. Under base push-out condition, the space-charge region will extend from the base-collector to the collector-subcollector interface, resulting in an effective widening of the neutral base region into the metallurgical collector. Consequently, no ohmic collector region remains. The length of the space-charge region, on the other hand, is rapidly reduced with increasing current, and the length criterion (1) will no longer be satisfied. With high collector doping, however, base push-out is reduced, and it has been shown in a theoretical study [6] that accumulation-layer mode operation is possible.

In order to obtain a pronounced Gunn effect it is proposed to insert an additional highly doped layer between base and collector [4]. This prevents base push-out and leads to a well defined space-charge region small in width. Based on this theory, it has been demonstrated [7], that a TED with a HBT-like layer structure shows oscillations at 77 GHz. This device in fact is an HBT with graded collector doping, that is operated in common base configuration at high current densities and a collector-base voltage below 1 V.

In this paper, it is shown — to the authors knowledge for the first time — that negative resistance effects may occur in high-voltage HBTs as well. These devices are designed for 2 GHz power amplifiers in base-stations (27 V bias voltage, [8]). The layer structures mainly consists of a 700 nm GaAs subcollector layer ($n = 5 \cdot 10^{18}$ cm^{-3}), a 2800 nm GaAs collector layer ($n = 4 \ldots 20 \cdot 10^{15}$ cm^{-3}), a 100 nm GaAs base layer ($n = 4 \cdot 10^{19}$ cm^{-3}), a 40 nm GaInP emitter layer ($n = 5 \cdot 10^{17}$ cm^{-3}), and GaAs and InGaAs contact layers. The collector of these devices is thick and weakly doped in order to obtain high breakdown voltages. As a consequence, the Gunn effect takes place in the space-charge region at base push-out. In common emitter configuration, this leads to $|S_{22}|$ exceeding unity. On the one hand, this effect is important for oscillator applications. On the other hand, although it is observed only at low voltages, it may affect the high-voltage power amplifier mode as well, since the trajectory includes the high current – low voltage region. However, it is not expected to lead to instability problems since it occurs at frequencies well beyond the common range of operation where circuit loss will suppress any instabilities.

Since the effect depends on collector thickness and doping as well as on bias point, HBTs with different collector dopings of $N_c = 4 \cdot 10^{15}$ (type A), $6 \cdot 10^{15}$ (type B), $8 \cdot 10^{15}$ (type C), and $2 \cdot 10^{16}$cm^{-3} (type D) are investigated. The effect appears most clearly in small-signal equivalent circuit modeling. Accordingly, its impact on circuit topology and element description is discussed as well.

0-7803-6540-2/01/$10.00 (C) 2001 IEEE

II. Results

A. S-Parameters

Typical S-parameters of an HBT with Gunn effect are shown in Fig. 1. In this measurement up to 100 GHz, it is observed that the magnitude of the output reflection coefficient S_{22} becomes larger than unity in a certain frequency range. It is a resonant behaviour that depends on bias point and collector doping.

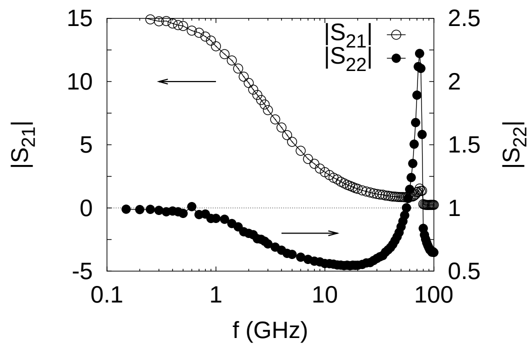

Fig. 1. $|S_{21}|$ and $|S_{22}|$ of $1(3 \times 30)\mu\mathrm{m}^2$ HBT, $N_c = 8 \cdot 10^{15}$ at $V_{ce} = 2\,V$, $I_c = 27\,\mathrm{mA}$, $f = 50\,\mathrm{MHz} \ldots 100\,\mathrm{GHz}$. It shows the typical $|S_{22}| > 1$ behaviour due to Gunn effect ($f = 56 \ldots 78\,\mathrm{GHz}$).

From theory it is expected that the Gunn effect sets in at the same current density as the Kirk effect. This is also observed in the S-parameters. The empty symbols in Fig. 2 show the transit frequencies at a fixed collector-emitter voltage $V_{ce} = 3\,V$ as a function of collector current. As expected the Kirk effect, that leads to the $1/I_c$ drop in f_t, sets in at higher currents for HBTs with higher N_c. In this figure, the solid symbols represent the frequency at which $|S_{22}| > 1$ reaches its maximum. This frequency will be referred to as resonance frequency due to Gunn effect. It is directly extracted from the S-parameter measurements without interpolation. It is observed that the Gunn and Kirk effects set in at the same collector current. The Gunn effect is observed up to very high currents, and is not immediately suppressed by base push-out. In the measurements shown here, the Gunn effect vanishes completely only for the lowest collector doping value, while it is still visible up to the maximum measured current for the other types of HBTs. At the same collector-emitter voltage, resonance frequency increases with collector doping.

For higher collector dopings, the maximum $|S_{22}|$ value is reached not only at higer currents, but also at higher voltages. Additionally, the magnitude increases from $|S_{22}| = 1.5$ at $I_c = 11\,\mathrm{mA}$, $V_{ce} = 2\,\mathrm{V}$ for type A to $|S_{22}| = 15.7$ at $I_c = 66\,\mathrm{mA}$, $V_{ce} = 5\,\mathrm{V}$ for type D. The maximum frequency is obtained at $V_{ce} = 1.5\,\mathrm{V}$ at the onset of the Kirk effect. It increases from 74 GHz for the lowest to a value

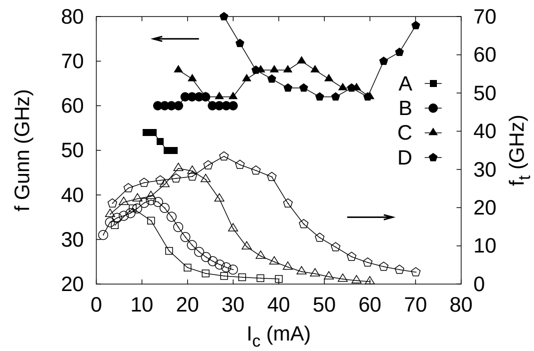

Fig. 2. Transit frequency f_t (empty symbols) and frequency of resonance due to Gunn effect (solid symbols) at $V_{ce} = 3\,V$ as a function of current. Parameter is collector doping, type A: $N_c = 4 \cdot 10^{15}\mathrm{cm}^{-3}$, type B: $N_c = 6 \cdot 10^{15}\mathrm{cm}^{-3}$, type C: $N_c = 8 \cdot 10^{15}\mathrm{cm}^{-3}$, type D: $N_c = 2 \cdot 10^{16}\mathrm{cm}^{-3}$.

larger than 100 GHz for the highest doping.

Bias dependence of the resonance is shown in Figs. 3 and 4. As expected from physics, the effect shows a maximum near the onset of the Kirk effect, and is reduced with increasing current. A wider space-charge region due to higher V_{ce} leads to a drastical decrease in resonant frequency. Also the maximum value of $|S_{22}|$ is reduced.

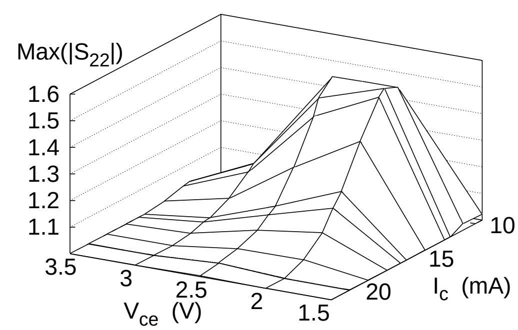

Fig. 3. Bias dependence of maximum value of $|S_{22}|$ for HBT type A ($N_c = 4 \cdot 10^{15}\mathrm{cm}^{-3}$).

B. Small-Signal Equivalent Circuit

In MESFETs, the Gunn effect is caused by the drain-source voltage and modulates the small-signal admittance Y_{ds} between drain and source. In HBTs, on the other hand, the Gunn effect in the collector does not depend mainly on base-collector voltage, but on collector current. Therefore, it is observed that not only base-collector admittance Y_{bc}, but also current gain α is affected. This reflects the fact that the voltage in the non-depleted (resistive) part of the collec-

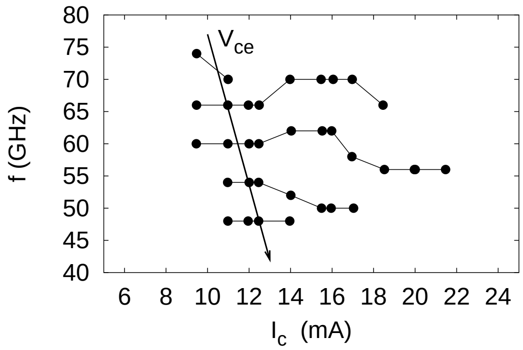

Fig. 4. Bias dependence of resonance frequency due to Gunn effect for HBT type A ($N_c = 4 \cdot 10^{15}\text{cm}^{-3}$). $V_{ce} = 1.5 \ldots 3.5$ V. The frequencies are measured in steps of 2 GHz.

tor, as well as the number of electrons in the space-charge region, is caused by I_c, which is given by αI_e.

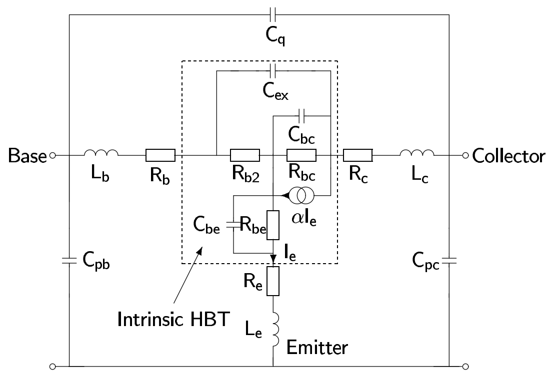

Fig. 5. Small-signal equivalent circuit of the HBT.

The small-signal equivalent circuit is shown in Fig. 5. After deembedding of the parasitics, α is determined from the intrinsic Y-parameters [9]:

$$\alpha = \frac{Y_{21} - Y_{12}}{Y_{11} + Y_{21}} \tag{3}$$

Typical values for α are shown in Fig. 6. For low currents, α shows its well-known low-pass characteristics. When the Gunn effect is observed, α exhibits a resonant behavior with a high maximum value, similar to the situation observed in S_{22}. For high currents, Gunn effect is canceled out by the Kirk effect. The common frequency-dependent model for α

$$\alpha = \frac{\alpha_0 e^{-j\omega\tau}}{1 + j\omega/\omega_\alpha} \tag{4}$$

with the parameters α_0, τ, and ω_α fails in this case. The polynomial

$$\alpha = \alpha_0 \frac{1 - j\omega\tau - \omega^2\tau^2/2}{1 + j\omega/\omega_\alpha - \omega^2/\omega_2 - j\omega^3/\omega_3} \tag{5}$$

is therefore applied to describe the behaviour. While the low-pass parameter ω_α remains unchanged, the exponential term is approximated by $e^x \approx 1 + x + x^2/2$. The terms related to ω_2 and ω_3 are inserted to account for the resonance and to assure that the high-frequency limit of α is zero. Fittings obtained with this formula for all three cases, low current, Gunn effect, and Kirk effect, are shown in Fig. 6.

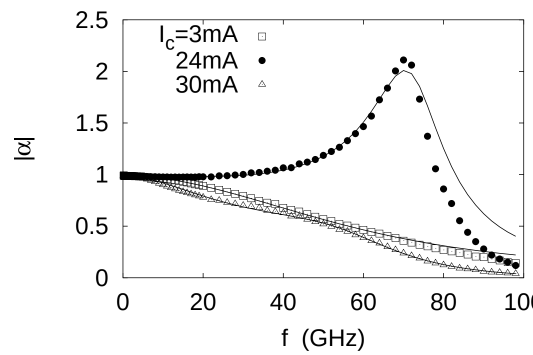

Fig. 6. Current dependence of magnitude of current gain $|\alpha|$ for HBT type C ($N_c = 8 \cdot 10^{15}\text{cm}^{-3}$); $f = 150\,\text{MHz} \ldots 100\,\text{GHz}$, $V_{ce} = 1.5$ V; Symbols: extracted values, lines: model.

In order to determine the base-collector admittance Y_{bc}, the intrinsic base resistance R_{b2} is extracted following the algorithm given in [9]. Then, the following equation is applied:

$$Y_{bc} = \frac{Y_{22} + Y_{12}}{Y_{11} + Y_{21}} \cdot \frac{1}{R_{b2}} \tag{6}$$

with $R_{b2} = 5\,\Omega$ for the HBTs under test.

While the Gunn effect is of major influence on α even at low frequencies, $\text{Im}(Y_{bc})$ shows a purely capacitive behaviour up to the frequency of resonance. In Fig. 7, it is shown that $\text{Im}(Y_{bc})$ for all currents exhibits a fairly linear behaviour up to 60 GHz, that can be modeled by $Y_{bc} = j\omega C_{bc}$, although the slope of the curves depends on current. In order to determine the real part of Y_{bc}, it is advantagous to use Z-parameters. After deembedding of C_{ex} from the intrinsic equivalent circuit, Y_{bc} is determined by

$$1/Y_{bc} = Z'_{22} - Z'_{21} \tag{7}$$

The real part of Y_{bc} is plotted in Fig. 8. In absence of the Gunn effect, $\text{Re}(Y_{bc})$ has a positive value. In case of the Gunn effect, it becomes negative, with a resonance at the same frequency as α. This behaviour is similar to that observed for Y_{ds} in MESFETs. At high current, when the Gunn effect is no longer observed in S_{22}, $\text{Re}(Y_{bc})$ still is slightly negative up to a frequency that corresponds to a small maximum in α.

The frequency dependence is modeled by

$$Y_{bc} = \frac{G_0 + j\omega C_0 - \omega^2 Y_1 - j\omega^3 Y_2}{1 + j\omega Y_3 - \omega^2 Y_4} \tag{8}$$

which can be understood as a chain of three $R_{bc}|C_{bc}$ branches.

In Fig. 9, modeled and measured S-paramters are shown for the HBT type A, in the bias point with maximum $|S_{22}|$. The agreement is good up to frequencies beyond the resonance due to Gunn effect.

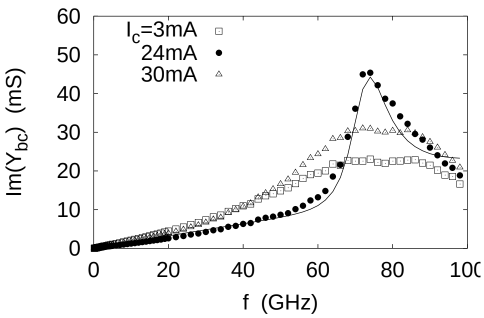

Fig. 7. Current dependence of $\mathrm{Im}(Y_{bc})$ for HBT type C ($N_c = 8 \cdot 10^{15}\mathrm{cm}^{-3}$); $f = 150\,\mathrm{MHz} \ldots 100\,\mathrm{GHz}$, $V_{ce} = 1.5\,\mathrm{V}$; Symbols: extracted values, line: model.

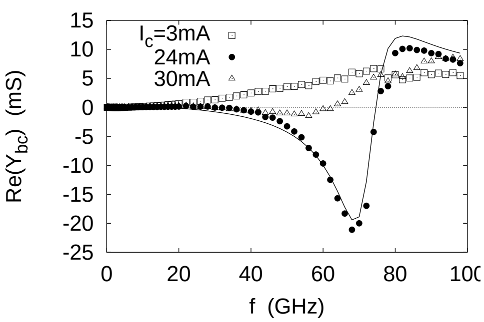

Fig. 8. Current dependence of $\mathrm{Re}(Y_{bc})$ for HBT type C ($N_c = 8 \cdot 10^{15}\mathrm{cm}^{-3}$); $f = 150\,\mathrm{MHz} \ldots 100\,\mathrm{GHz}$, $V_{ce} = 1.5\,\mathrm{V}$; Symbols: extracted values, line: model.

III. Conclusions

Negative resistance effects in high-voltage HBTs are reported. The Gunn effect in the thick collector region leads to $|S_{22}|$ exceeding unity for mm-wave frequencies. High currents in a wide collector region are necessary for this effect to occur. As expected from theory, it sets in together with the base push-out effect, which in turn suppresses the Gunn effect at high currents. For higher collector doping, the effect becomes stronger and is observed at higher voltages, currents, and frequencies.

In the small-signal model, the Gunn effect leads to a resonant behaviour of current gain α and base-collector admittance Y_{bc}. In contrast to its usual low-pass behaviour, $|\alpha|$ is found to increase beyond unity until it reaches the resonance

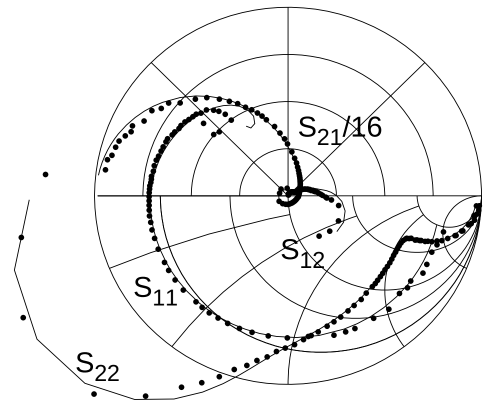

Fig. 9. Measured and modeled S-parameters of type A HBT ($N_c = 4 \cdot 10^{15}\mathrm{cm}^{-3}$); $f = 150\,\mathrm{MHz} \ldots 70\,\mathrm{GHz}$, $V_{ce} = 2\,\mathrm{V}$, $I_c = 13\,\mathrm{mA}$; Symbols: measurements, lines: model

frequency. Up to this frequency, Re(Y_{bc}) is negative. A simplified model for this behaviour is proposed to describe the S-parameters.

The effect may be exploited for oscillator applications and should be considered for a refined modeling.

Acknowledgments

The authors would like to thank the material and process technology departments of the FBH for providing the HBTs, S. Schulz for performing measurements, and Dr. W. Heinrich for helpful discussions and continous encouragement.

References

[1] S. M. Sze, *Physics of Semiconductor Devices*, New York: J. Wiley & Sons, 1981, p. 652.

[2] T. A. Fjeldly, ”Analytical modeling of the stationary domain in GaAs MESFET's”, *IEEE Trans. Electron Dev.*, vol. 33, No. 7, pp. 874 – 880, 1986.

[3] F. Lenk, R. Doerner, P. Heymann, ”Negative resistance in GaAs MESFET nonlinear modeling”, in: *Dig. 4th. INMIC*, Duisburg, Germany, pp. 77 – 82, 1996.

[4] V. A. Posse, B. Jalali, ”Novel transient phenomena in heterojunction bipolar transistors”, *Solid State Electron.*, vol. 41, No. 4, pp. 527 – 530, 1997.

[5] R. J. Whittier, D. A. Tremere, ”Current gain and cutoff frequency falloff at high currents”, *IEEE Trans. Electron Dev.*, vol. 16, No. 1, pp. 39 – 57, 1969.

[6] C. Dalle, M. R. Friscourt ”Bipolar cathode transferred-electron device for millimeter-wave generation”, *Solid State Electron.*, vol. 44, No. 1, pp. 79 – 84, 2000.

[7] J. K. Twynam, M. Yagura, N. Takahashi, E. Suematsu, H. Sato, ”Demonstration of a 77-GHz heterojunction bipolar transferred electron device”, *IEEE Electron Dev. Lett.*, vol. 21, No. 1, pp. 2 – 4, 2000.

[8] P. Kurpas et. al., ”High-Voltage GaAs Power-HBTs for Base-Station Amplifiers”, in: *IEEE MTT-S Int. Microwave Symp. Dig.*, 2001, WE1B-1.

[9] M. Rudolph, R. Doerner, P. Heymann, ”Direct extraction of HBT equivalent circuit elements”, *IEEE Trans. Microwave Theory Tech.*, vol. 47, No. 1, pp. 82 – 84, 1999.